MEMBRANE ASYMMETRY AND ENHANCED ULTRASTRUCTURAL DETAIL OF SARCOPLASMIC RETICULUM REVEALED WITH USE OF TANNIC ACID

AKITSUGU SAITO, CHENG-TEH WANG, and SIDNEY FLEISCHER

From the Department of Molecular Biology, Vanderbilt University, Nashville, Tennessee 37235

ABSTRACT

Fixation of purified sarcoplasmic reticulum (SR) membrane vesicles, using glutaraldehyde supplemented with 1% tannic acid, reveals newly visualized ultrastructure in thin sections. The trilaminar appearance of the membrane is highly asymmetric; the outer electron-opaque layer is appreciably wider (70 Å) than the inner layer (20 Å). The asymmetry is not referable to lack of penetration of the tannic acid since: (*a*) SR vesicles made permeable with 1 mM EDTA, pH 8.5, show similar asymmetry; (*b*) treatment of SR with trypsin results in progressive loss in protein content and decrease in the thickness of the outer layer, until in the limit the trilayer has a symmetric appearance; (*c*) within the same muscle section, the SR membrane appears highly asymmetric whereas the sarcolemma has a more symmetric appearance; (*d*) reconstituted SR vesicles have a symmetric appearance with equally broad inner and outer layers (~70 Å); the symmetric structure is confirmed by freeze-fracture and negative staining electron microscopy. Heavy and light SR vesicles obtained by isopycnic density sedimentation of purified SR have the same asymmetric appearance of the membrane and seem to differ mainly in that the heavy vesicles contain internal contents consisting largely of Ca^{++}-binding protein. The asymmetry of the SR membrane is referable mainly to the unidirectional alignment of the Ca^{++} pump protein, the major component (90% of the protein) of the membrane. The asymmetry of the SR membrane can be visualized now for the first time *in situ* in thin sections of muscle.

KEY WORDS sarcoplasmic reticulum · tannic acid · membrane asymmetry · molecular detail · Ca^{++} pump protein · membrane ultrastructure

Tannic acid fixation was introduced by Mizuhira and Futaesaku in 1971 (30) and has been used to enhance electron density in a variety of cellular structures, including microtubules (1, 10, 31, 41), microfilaments (19), membranes (15) and membrane surface structures (32, 36), and membrane junctions (2, 4, 42) when used in conjunction with glutaraldehyde and OsO_4.

We have used tannic acid together with glutaraldehyde and postfixation with osmium tetroxide for visualization of sarcoplasmic reticulum (SR), both *in situ* and in purified preparations. We find that this method provides new definition regarding the asymmetry of SR as well as generally enhanced contrast of muscle which is otherwise not

readily visible in thin sections. A preliminary report has appeared (37).

MATERIALS AND METHODS

Electron Microscopy

THIN SECTIONS, FIXATION, AND EMBEDDING: Samples were fixed in 2.5% glutaraldehyde in 0.1 M sodium cacodylate buffer (pH 7.2) containing 1% tannic acid (Mallinckrodt analytical reagent [Mallinckrodt Inc., St. Louis, Mo.]) for 2 h at 4°C and postfixed in 1% OsO_4 in 0.1 M veronal-acetate buffer (pH 7.2), 2.4 mM $CaCl_2$, and 0.06 M NaCl for 2 h at 4°C (tannic acid-glutaraldehyde-OsO_4). Rabbit skeletal muscle tissue was fixed as small cubes, ~0.3–0.5 mm on a side. Isolated SR vesicles were fixed either in suspension or as pellets. Some of the samples were fixed in 2.5% glutaraldehyde for 2 h at 4°C and then postfixed in 1% OsO_4 in 0.1 M cacodylate buffer pH 7.2 (glutaraldehyde-OsO_4). All samples were block-stained with 0.5% uranyl acetate in veronal-acetate buffer (pH 6.0) for 2 h at room temperature, dehydrated in a series of increasing ethanol concentrations, the ethanol was replaced with propylene oxide, and the samples were embedded in Epon 812 (7). Thin sections were cut on an LKB Ultratome (LKB Instruments, Inc., Rockville, Md.), stained with 1% uranyl acetate in 50% ethanol for 10 min, counterstained with lead citrate (38), and examined in a Hitachi HU-11B electron microscope.

NEGATIVE STAINING: Negative staining with 2% phosphotungstic acid (pH 7.2) or 1% uranyl acetate was carried out as described previously (7).

FREEZE-FRACTURE: Freeze-fracture and preparation of the replicas was carried out in a Balzers BAF 300 apparatus (Balzers High Vacuum Corp., Santa Ana, Calif.) in a manner previously described (3). The isolated SR vesicles, ~0.5–1.0 mg, were sedimented into pellets, covered with a solution of 25% glycerol in 0.3 M sucrose, 1 mM *N*-2-hydroxyethylpiperazine-*N'*-2-ethanesulfonic acid (HEPES), 100 mM KCl (pH 7.2), and left to soak for 3–12 h in the cold. The specimens were fractured at a vacuum of 6×10^{-7} Torr at −100°C and shadowed with 20 Å platinum-carbon at an angle of ~45° and carbon. The replicas were floated onto 5% Clorox for 5 min and cleaned with distilled water.

MICRODENSITOMETRY: A microdensitometer, Photometric Data Systems (Perkin Elmer Ultek, Inc., Palo Alto, Calif.; Model 1050), was used to scan the photographic plates obtained by electron microscopy. Each scan consisted of 500 optical density readings, made at 2-μm intervals across the image of the membrane. The slit was 16×170 μm. A magnification of 20 was used. The scans are shown from the inside of the vesicle or cell to the outside. The widths of the layers of the trilayer were calculated from the half-heights.

Preparation of SR Vesicles

SR vesicles were purified by zonal centrifugation as previously described (25), except that HEPES buffer was deleted from the homogenization buffer and the sucrose gradient solutions. The purified SR was then subfractionated into light and heavy SR as previously described (29).

Trypsin Treatment of SR Vesicles

Trypsin digestion of SR was carried out in an ice bucket at 0°C in 1-ml reaction mixture containing 1 mg of SR protein, 0.2 mg of trypsin, 26% sucrose, 5 mM HEPES (pH 7.1), and 100 mM KCl. This is a slow trypsin digestion as compared with those reported previously (12, 13, 39) in which digestion was carried out at room temperature. The reaction was stopped by introducing trypsin inhibitor (0.4 mg of protein/ml) after incubating for varying periods of time as indicated in the legends of Figs. 2 and 4. The samples were washed twice with a solution containing 0.3 M sucrose, 100 mM KCl, and 5 mM HEPES (pH 7.1), and then suspended in 0.3 M sucrose, 100 mM KCl, and 5 mM HEPES (pH 7.1).

EDTA Extraction of SR Vesicles

SR vesicles (10 mg of protein) were extracted several times at 0°C with 8 ml of a solution containing 1 mM EDTA, 10 mM Tris-HCl (pH 8.5). The alkaline, hypotonic EDTA treatment, originally described by Duggan and Martonosi (5), makes the SR membrane porous so that internal contents leak out (29). The final pellet was suspended in 0.3 M sucrose, 100 mM KCl, 1 mM HEPES at pH 7.1

Assays

Total phosphorus was measured as an estimate of lipid phosphorus (24). Protein was determined by the procedure of Lowry et al. (21) with bovine plasma albumin as a standard.

The Ca^{++} loading rate and Ca^{++}-stimulated ATPase activity were determined at 23°C in the same medium containing 0.1 M KCl, 5 mM $MgCl_2$, 5 mM ATP, 100 μM $^{45}Ca^{++}$, 5 mM oxalate, and 10 mM HEPES, pH 7.0. Ca^{++} loading was initiated by the addition of ATP and was sampled after 1 min by filtration (type GS 0.22 μM Millipore filter [Millipore Corp., Bedford, Mass.]) (25). The decrease in ^{45}Ca in the filtrate was used to calculate the calcium loading activity. The Ca^{++}-stimulated ATPase was measured at 1 min of reaction. Inorganic phosphate was determined by the procedure of Fiske and Subbarow (6) with Elon as a reducing agent.

Polyacrylamide Gel Electrophoresis

The protein profile of SR preparations was obtained by polyacrylamide gel electrophoresis in 0.1% sodium dodecyl sulfate (SDS) gels containing 11% and 5% acrylamide in the separating and stacking gels, respec-

tively, and were prepared and run as described by Laemmli (17). Gels were stained with 1% Amido Black in 9% acetic acid and 50% methanol for 10 h. They were destained by soaking in several changes of 10% acetic acid and 20% methanol for several days.

RESULTS

Isolated SR Vesicles

Purified SR is isolated as sealed vesicles, and its appearance in thin sections reflects this. The trilaminar appearance of the membrane is readily observed. The membrane has a symmetrical appearance with OsO_4 fixation (Fig. 1 *a*). The widths of the three layers, measured by microdensitometry (Fig. 1 *d*) and calculated from the half-height of the bands, are 24, 16, and 26 Å from the inside to the outside of the membrane vesicle, a total width of 66 Å. With glutaraldehyde followed by osmium tetroxide fixation, some additional surface structure can be discerned, irregularly distributed around the outer layer of the vesicle membranes (see Fig. 1 *b*). While the widths of the inner and middle layers of the trilaminar membrane are the same as for osmium tetroxide fixation alone (Fig. 1 *a*), the thickness of the outer layer varies and, in places, approaches 70 Å (cf. Fig. 1 *b*, note arrow). However, the general appearance of the outer layer is only somewhat more asymmetric than in the case of OsO_4 fixation alone. When tannic acid is used in addition to glutaraldehyde followed by osmium tetroxide, there is enhanced contrast revealing a uniform dense outer band of the trilayer (see Fig. 1 *c*). The thickness of the membrane bands of the trilayer obtained by densitometry is 22, 21, and 70 Å, from the inside to the outside of the membrane vesicle, i.e., a total width of 113 Å (Fig. 1 *f*).

The membrane asymmetry, which is observable with tannic acid, is lost after tryptic digestion (Fig. 2). The progressive degradation was readily followed by digestion at 0°–2°C. A particulate fraction was recovered by sedimentation after varying time intervals. There is a gradual loss of protein and Ca^{++} loading rate with increased time of digestion and a concomitant increase in membrane-bound Ca^{++} ATPase activity over this time interval (Table I). Progressively longer treatment with trypsin results in decreased thickness of the outer layer of the SR membrane (Fig. 2). The membrane thickness of the trypsin-digested SR vesicles decreases with the time of digestion, and in the limit little or no asymmetry remains. The microdensitometer tracing at this time-point shows a symmetric membrane (Fig. 2 *c* and *d*). After 24 h of digestion, the surface layer is no longer uniform in thickness (Fig. 2 *a*); the maximum thickness observed was 70 Å, the same as for untreated vesicles. After 72 and 120 h, the measurement is 40 and 25 Å, respectively (Fig. 2 *b* and *c*, respectively). The thickness of the middle and inner layers remained unchanged from that in untreated vesicles (20 and 25 Å, respectively). After 120 h of digestion there is: (*a*) essentially no Ca^{++} uptake activity left; (*b*) a doubling of Ca^{++}-stimulated ATPase activity; (*c*) complete degradation of Ca^{++} pump protein to smaller peptides of which three remain particulate-bound, i.e., 50,000, 30,000, and 20,000 daltons (gel *D*, Fig. 4); (*d*) loss of most of the membrane asymmetry as viewed by tannic acid fixation (Fig. 2 *c*). Tryptic digestion also results in the loss of visualization of the 40-Å particles which are observed on the outer surface of the SR membrane by negative staining (Fig. 3 *a* and *b*).

The Ca^{++}-binding protein is normally localized within the compartment of heavy SR vesicles (29) (see also references 11, 39, 40, 44). The loss of the Ca^{++}-binding protein from the trypsin-treated SR as monitored by SDS gel electrophoresis (Fig. 4) indicates that the membranes have been made leaky.

Tannic Acid Fixation of Leaky SR Vesicles

It might be argued that the asymmetric appearance of the SR membrane, visualized by tannic acid fixation, may be an artifact due to failure of tannic acid to penetrate the SR membrane vesicle to the inner surface. If that were so, the asymmetry would have a trivial explanation rather than reflecting membrane asymmetry. This possibility was tested by using SR membranes made leaky by treatment with 1 mM EDTA buffered at pH 8.5 (5, 29). Such vesicles appear broken open (Fig. 5) and have lost their inner contents, i.e., Ca^{++}-binding protein (29) (compare Figs. 5 and 9 *e*). These leaky vesicles have lost their ability to pump Ca^{++} while the ATPase activity doubled (not shown). The leaky vesicles have the same asymmetric appearance with tannic acid fixation as normal SR membrane vesicles. Thus, the observed asymmetry is a real characteristic of the SR membrane.

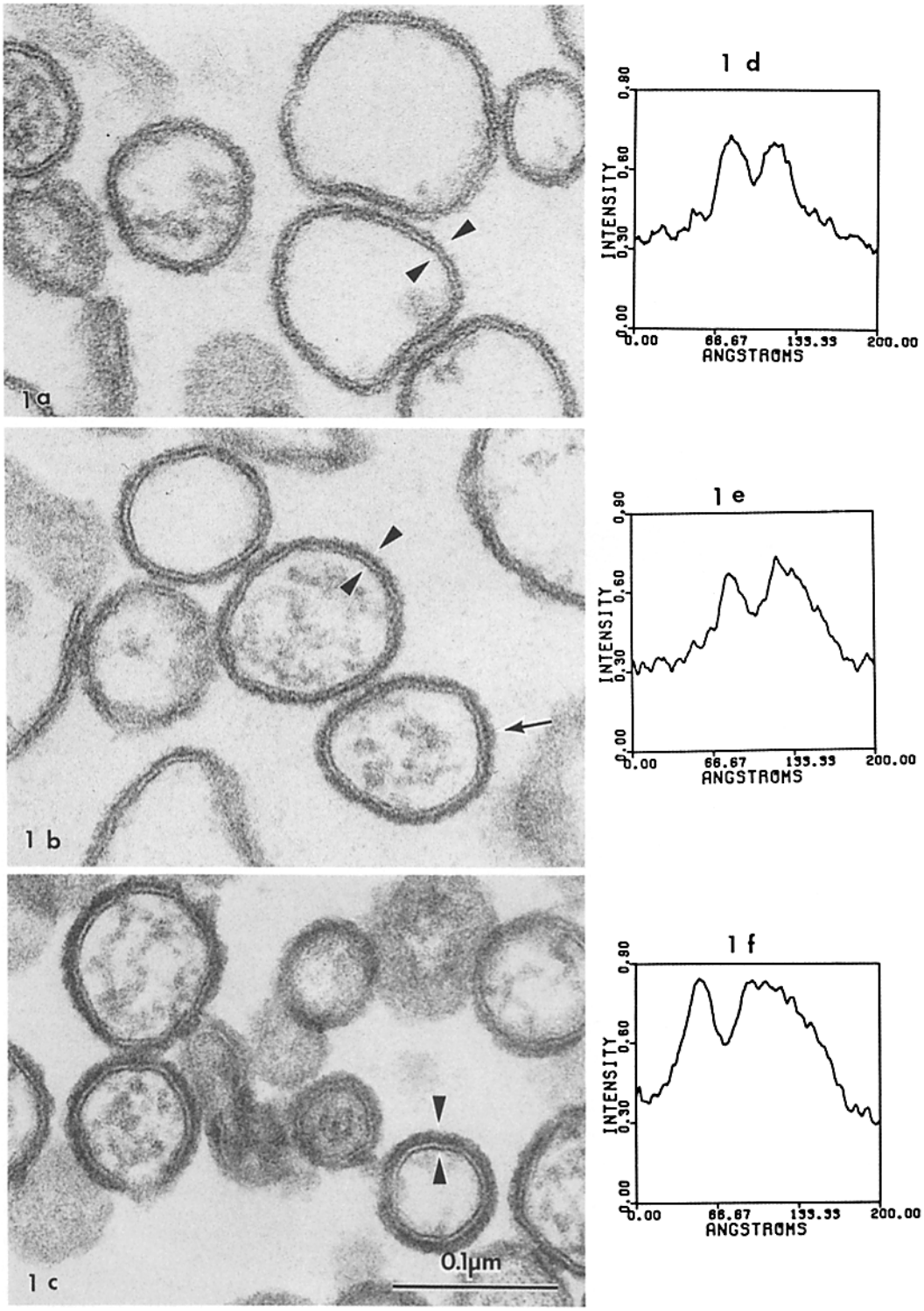

FIGURE 1 Isolated vesicles of SR observed in thin sections using three different fixation procedures (× 250,000). (*a*) Fixation with OsO_4 alone. The widths of membrane trilayer, from the inside of the vesicle to the outside, are 24, 16, 26 Å, i.e., a total width of 66 Å. (*b*) Fixation with glutaraldehyde-OsO_4. The widths of membrane trilayer at the points indicated are: 19, 22, 50 Å. The arrow points to a region where the width of the outer layer approaches 70 Å. (*c*) Fixation with tannic acid-glutaraldehyde-OsO_4 (see Materials and Methods for procedures). Note enhanced density of outer layer. The widths of membrane trilayer are: 22, 21, 70 Å. (*d–f*) Microdensitometer tracings of Fig. 1 *a–c*, respectively. The arrowheads in Fig. 1 *a–c* indicate the region which was scanned. The widths of each layer of the trilayer were measured from the half-height of the microdensitometry scans.

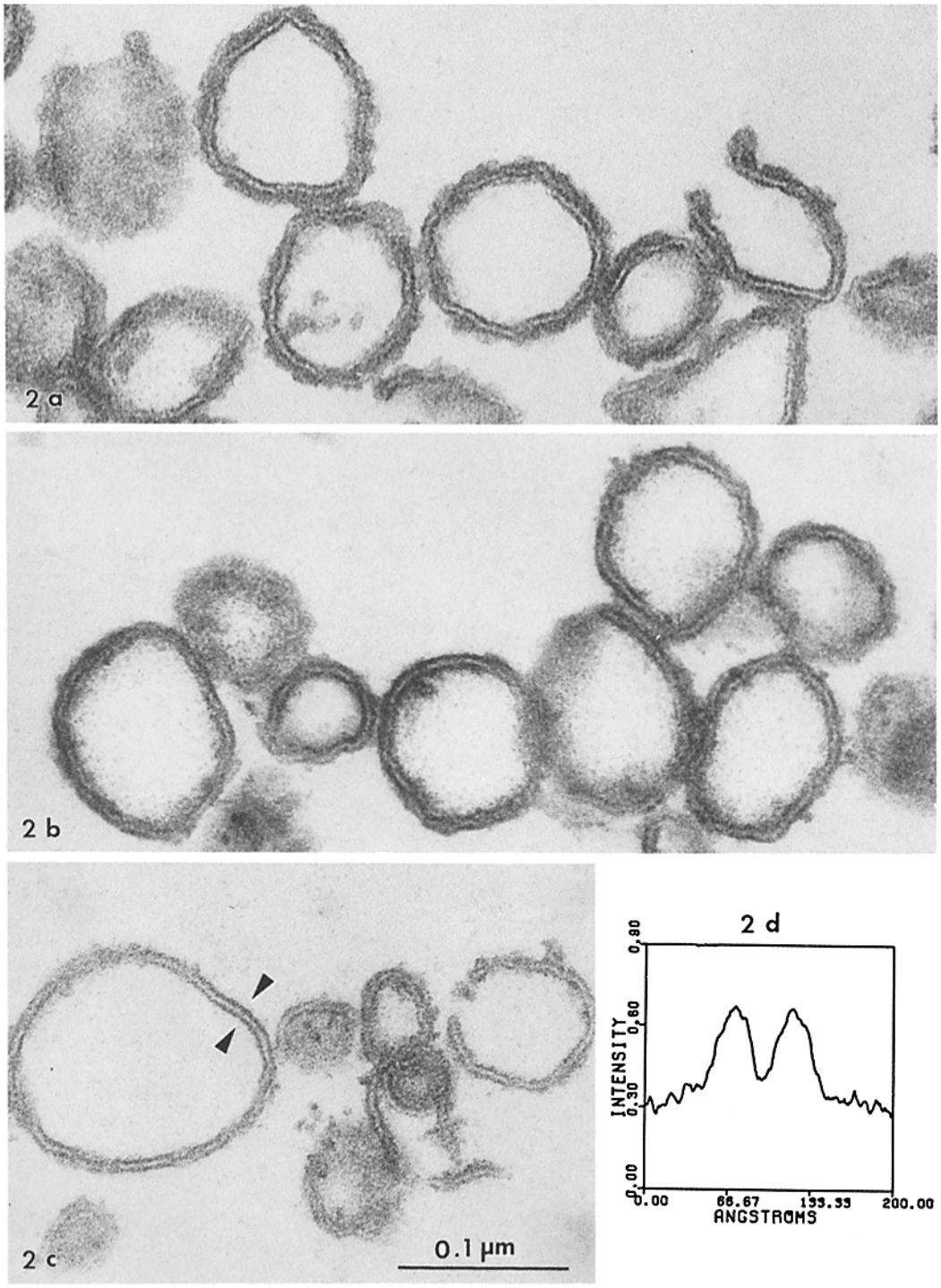

FIGURE 2 Isolated vesicles of SR treated with trypsin for varying periods of time. Digestion with trypsin was carried out at 0°C for (*a*) 24 h, (*b*) 72 h, (*c*) 120 h, respectively. The fixative contained tannic acid. Note successive decrease in width of outer layer of the membrane with duration of digestion (× 250,000). (*d*) The microdensitometer tracing of Fig. 2*c* was made between the points indicated on the micrograph. The widths of the bands of the trilayer were 24, 20, 24 Å.

TABLE I

Properties of Sarcoplasmic Reticulum Vesicles Digested with Trypsin

Sample	Control SR	A	B	C	D
Time period of trypsin digestion (h)	0	1	24	72	120
Lipid content (μmol P/mg protein)	0.75	0.76	0.81	0.88	1.11
Loss of protein from SR (%)	0	1.02	6.85	14.35	32.36
Ca^{++} loading rate (μmol Ca^{++}/mg protein/min)	2.08	2.04	1.04	0.15	0.03
ATPase rate (μmol Pi/mg protein/min)	1.09	1.13	1.55	1.81	1.92
Loading efficiency (Ca^{++}/ATP)	1.91	1.81	0.67	0.08	0.015

SR vesicles were digested with trypsin at 0°C for varying periods of time as described in Materials and Methods. The protein profile in membrane fractions is shown in Fig. 4. Control SR was stored at 0°C for 120 h without added trypsin.

Reconstituted SR Membrane Vesicles

SR can be dissociated and reconstituted to form functional membrane vesicles with a phospholipid to protein composition similar to that of normal SR (28). Tannic acid fixation of such reconstituted vesicles reveals a symmetric membrane with broad (70 Å wide) inner and outer bands (Fig. 6*b* and *c*) of high contrast. There is heterogeneity of membrane appearance in the reconstituted vesicles. ~25% of the vesicles have a broad continuum with dense outer and inner bands (cf. Fig. 6*c*). The thickness of the three bands of the trilayer are 72, 24, and 72 Å as determined by densitometry (Fig. 6*e*). The remainder of the reconstituted vesicles have broadened patches on both outer and inner bands of the membrane instead of a continuum (cf. Fig. 6*b*). The reconstituted vesicles fixed with tannic acid (Fig. 6*b* and *c*) can be contrasted with those fixed with glutaraldehyde in the absence of tannic acid (Fig. 6*a*) where the lack of contrast is apparent. Freeze-fracture electron microscopy of the same preparation of reconstituted SR membrane vesicles is included (Fig. 7) and confirms the symmetric orientation as compared with normal SR where the particles are mainly on the outer fracture face (3).

The symmetric orientation of reconstituted SR vesicles is further confirmed by negative staining. The 40-Å particles observed in normal SR only on the outer surface (Fig. 3*a* and *d*) (12) can be visualized on both outer and inner surfaces in the reconstituted preparation (Fig. 3*c* and *e*). The width of the reconstituted SR membrane measured from the negatively stained membrane is comparable with that measured in thin sections using tannic acid to obtain enhanced contrast (compare Figs. 1*c* and 3*e*).

In other studies, we find that as the phospholipid to protein ratio of the reconstituted SR vesicles is increased, the patches get smaller and are further apart and most of the surface lacks the broadened mass on the outer and inner bands of the membrane.[1] The fact that reconstituted SR shows a broadened outer and inner band of the membrane means that tannic acid permeates the SR membrane and reflects asymmetry where it exists. Reconstituted SR vesicles are symmetric, having broad inner and outer bands (70 Å wide) (Figs. 6*c* and *e*).

Muscle Tissue

Tannic acid can thus be used to visualize membrane asymmetry in isolated SR membrane vesicles. The procedure was next applied to muscle tissue. Rabbit skeletal muscle fixed with glutaraldehyde with and without tannic acid exhibits comparable good morphology (compare Figs. 8*a* and 9*a*). At higher magnification, the effect of tannic acid as a fixative for SR is impressive. There is a striking enhancement of overall contrast and a profound asymmetry in the SR membrane (compare Fig. 8*b* with *d* and Fig. 9*b* with *d*). The cytoplasmic layer is 70 Å wide as compared with 20 and 22 Å for the mid- and luminal bands of the trilayer, respectively. The total width of the trilaminar membrane is 112 Å (Fig. 8*e*). The widths of the membrane bands in the absence of tannic acid are 20, 20, 20 Å, respectively, a total width of 60 Å (Fig. 8*b*). The profound asymmetry of the SR membrane, which is revealed by tannic acid fixation, is not observed in the sarcolemma in the same field of the thin section (Fig. 8*f* and *g*). The SR junction with the sarcolemma membrane

[1] Wang, C.-T., A. Saito, and S. Fleischer. Correlation of ultrastructure of reconstituted SR membranes with changes in lipid and protein composition. Manuscript in preparation.

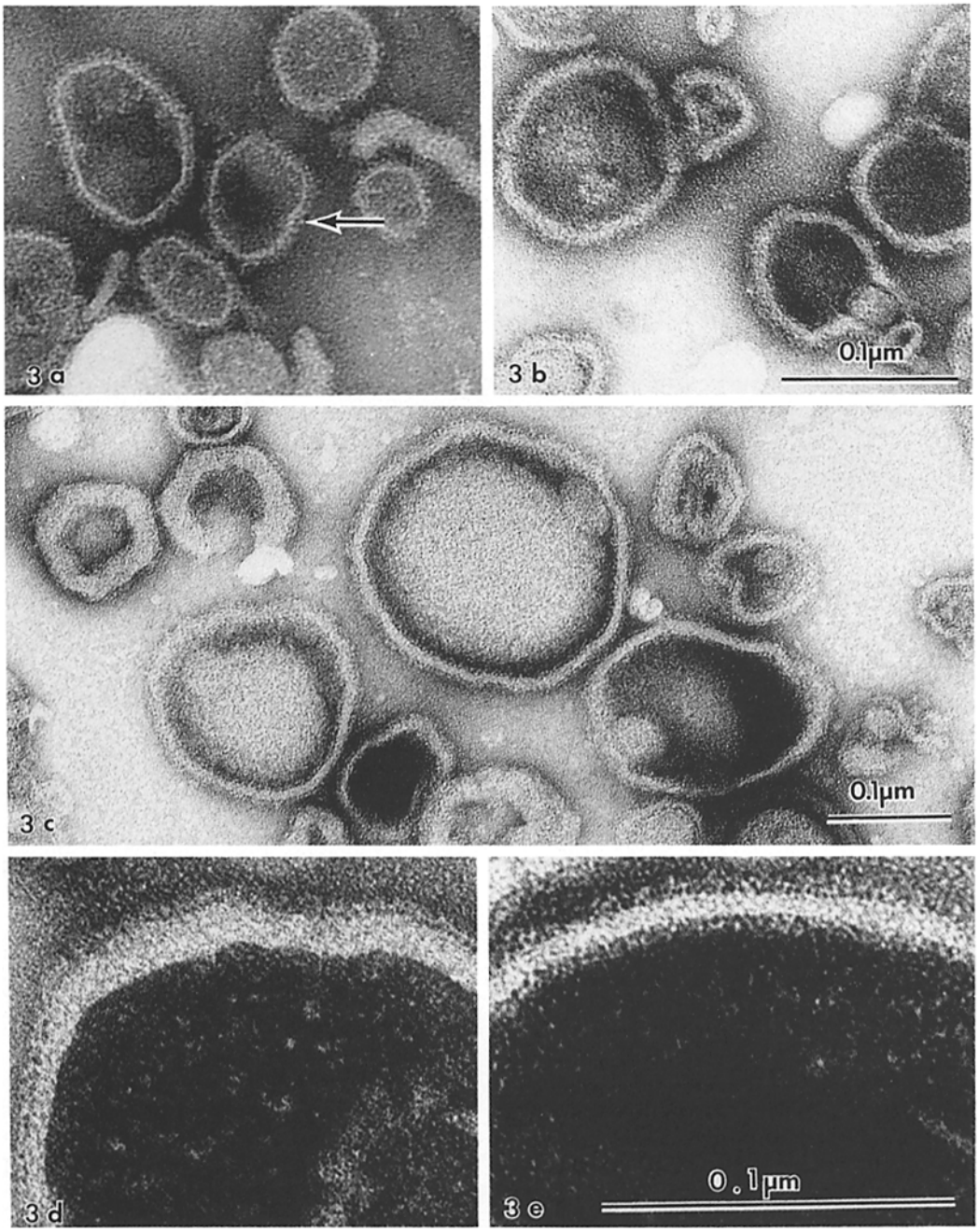

FIGURE 3 SR visualized by negative staining. (*a*) isolated SR vesicles, negatively stained with 2% phosphotungstic acid, pH 7.2. Particles ~40 Å in diameter can be observed on the outer surface of the membrane (arrow) (×250,000). (*b*) SR vesicles treated with trypsin for 72 h before negative staining (cf. legend, Fig. 2*b*). The particles are less readily detectable on outside of membrane. (*c*) Reconstituted SR vesicles negatively stained with 1% uranyl acetate (×175,000). The 40-Å particles can be visualized on both outer and inner surfaces (cf. Fig. 3*e* for higher magnification). (*d* and *e*) Higher magnification of normal and reconstituted SR membrane vesicles, respectively, negatively stained with 1% uranyl acetate (×500,000). In normal SR membranes, the particles can be visualized only on the outer surface of the membrane whereas the particles are visualized on both inner and outer surfaces of the reconstituted SR membrane. The minimal width of the reconstituted membrane including the surface particles is 160 Å, and probably reflects the true width of the membrane as observed by negative staining. To observe this minimal width of the membrane, the section must be well flattened and the stain must have adequately penetrated.

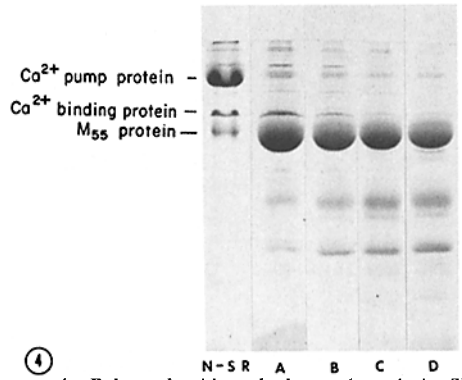

FIGURE 4 Polyacrylamide gel electrophoresis in SDS of isolated SR vesicles, before and after treatment with trypsin for varying periods of time. (*N-SR*) normal SR maintained for 120 h with no added trypsin. (Gels *A*, *B*, *C*, and *D*) SR vesicles treated with trypsin at 0°C, as described in the text, for 1, 24, 72, and 120 h, respectively (cf. also Table I).

is shown in Fig. 8*g*. Enhanced contrast of the junction granules (*JG*) can readily be observed.

The triad structure can be visualized with better definition in the tannic acid-fixed samples (compare Fig. 9*b* and *d*). The asymmetry of the SR membrane is notable especially as compared with the transverse tubule which has only a slight asymmetric appearance. The enhanced contrast permits clearer visibility of the junction granules at the SR-T-tubule junction (cf. Fig. 9*c*; compare Fig. 9*b* and *f*). Our studies with tannic acid, at present, do not permit us to resolve whether the junctional SR membrane, i.e., the region of the SR membrane facing the T-tubule, is different from the remainder of the SR membrane as indicated from the freeze-fracture studies of Franzini-Armstrong (9) (cf. Fig. 9*d*).

It may be noted that the terminal cisternae, i.e., the portion of the SR which forms a junction with

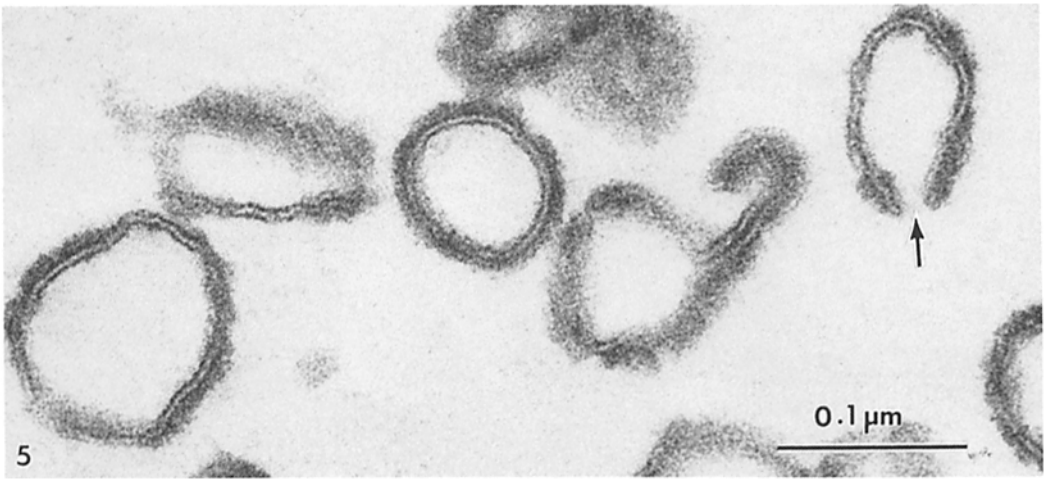

FIGURE 5 "Leaky" SR vesicles fixed with tannic acid-glutaraldehyde-OsO_4. The SR vesicles were made leaky by treatment (two washes) with 1 mM EDTA, pH 8.5, 0°C. The asymmetry of the membrane is clearly visible in the broken vesicles (see arrow). (×250,000). The contents of the vesicles have leaked out as a result of the treatment.

FIGURE 6 Reconstituted SR vesicles (see Materials and Methods). (×250,000). The reconstituted membrane vesicle preparation was heterogeneous and had a lipid phosphorus of 22 as compared with 30 μg P per milligram of protein for normal light SR vesicles. (*a*) Fixation with glutaraldehyde-OsO_4. (*b* and *c*) Fixation with tannic acid-glutaraldehyde-OsO_4. Note broadened outer and inner bands of the membrane in the reconstituted preparation. (*b*) In ~70% of the SR vesicles, the thick outer and inner layers of the membrane are discontinuous, as shown here (arrows point to patches of surface material) at this lipid-to-protein ratio. (*c*) A reconstituted vesicle is shown whose outer and inner membrane layers appear continuous. (*d*) Amorphous appearance of detergent-solubilized SR; SR was solubilized using deoxycholate as for reconstitution (28), but removal of detergent has not yet been carried out as in Fig. 6*a–c*. Fixation was with tannic acid-glutaraldehyde-OsO_4. (*e*) Densitometry tracing of Fig. 6*c*, between points indicated on the micrograph. Widths of membrane layers are 72, 24, 72 Å, respectively, or a total width of 168 Å. This total width is similar to that observed by negative staining (cf. Fig. 3*e*).

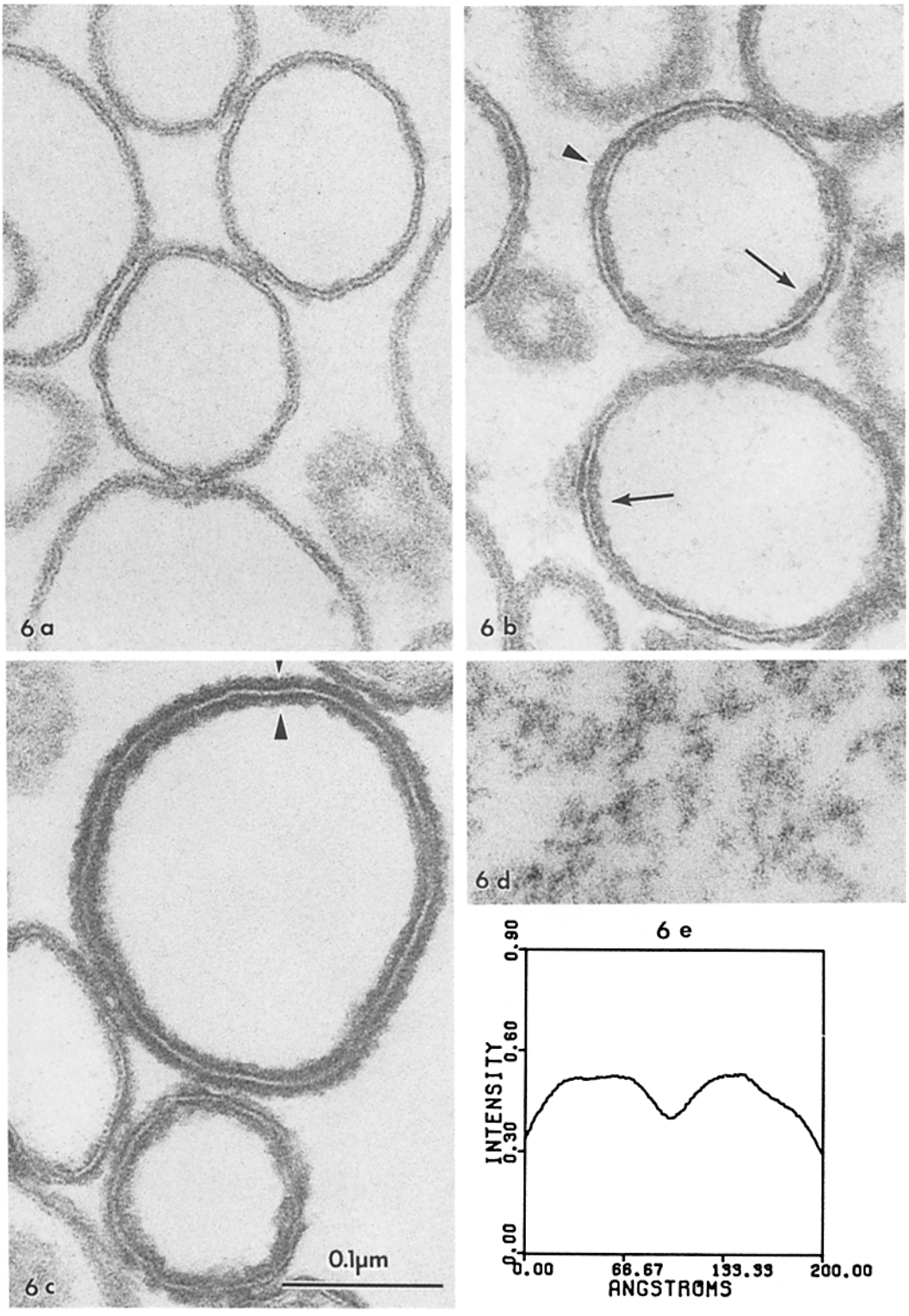
6 a
6 b
6 c
0.1μm
6 d
6 e
INTENSITY
0.90
0.60
0.30
0.00
0.00
66.67
133.33
200.00
ANGSTROMS

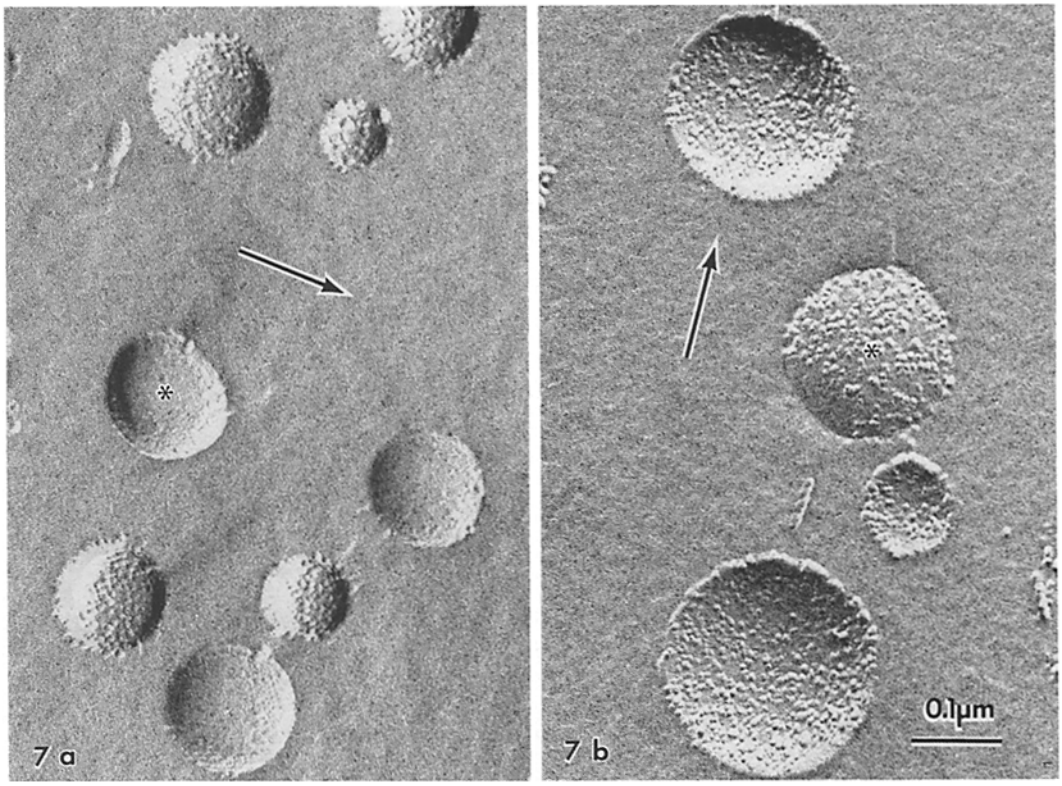

FIGURE 7 Isolated SR vesicles observed with the freeze-fracture technique of sample preparation. Arrows indicate direction of shadowing. Asterisks indicate convex regions (× 120,000). (*a*) normal SR vesicles showing asymmetry of particle distribution between outer and inner fracture faces as compared with reconstituted vesicles in Fig. 7*b*. The reconstituted vesicles are the same preparation used in Fig. 6*c*.

the transverse tubule, contains electron-opaque contents which can be better visualized with the use of tannic acid (compare Fig. 9*b* and *d*). The lateral cisternae of SR and the transverse tubule, by contrast, are devoid of electron-opaque contents (Fig. 9*d*).

We have previously reported that highly purified SR is heterogeneous with respect to the

FIGURE 8 Rabbit skeletal muscle in thin section with emphasis on ultrastructural detail of SR. (*a*) Longitudinal section of rabbit skeletal muscle, fixed with glutaraldehyde-OsO_4 (× 22,500). Compare with Fig. 9*a* in which the fixative contained also tannic acid. In both, the general morphology is well preserved. Sarcoplasmic reticulum (*SR*), transverse tubules (*TT*), and mitochondria (*M*) are indicated. Higher magnification is required to appreciate the superior definition and contrast made possible with the use of tannic acid. Ultrastructural detail can be seen in the SR in Fig. 8*b–g*. (*b*) Fixed with glutaraldehyde-OsO_4 (× 200,000). Fig. 8*c, d, f,* and *g* show muscle fixed with tannic acid-glutaraldehyde-OsO_4. The asymmetry of the SR membrane is revealed by fixation with tannic acid. (*c*) Two SR membranes in apposition are shown (arrow) (× 200,000). (*d*) The asymmetric structure of the SR membrane is clearly visible with tannic acid fixation (× 250,000). (*e*) Microdensitometer tracing of membrane in Fig. 8*d* between points indicated. The widths of the inner, middle, and outer layers of 22, 20, and 70 Å, respectively, as measured from the half-heights of the densitometry tracing. (*f*) A section of the sarcoplasmic reticulum (*SR*) is shown next to the sarcolemma (*SL*). Note the pronounced asymmetry seen in the SR membrane but not in sarcolemma; (*g*) SR-sarcolemma junction. Junction granules, denoted by arrowheads, can be seen between the junctional sarcoplasmic reticulum membrane (*JS*) and the sarcolemma (*SL*). *ECS* denotes extracellular space. The distance between the two membranes of the junction is 200 Å. (× 250,000).

luminal contents (25, 29). This heterogeneity can readily be visualized by electron microscopy in thin sections (Fig. 1*c*). The contents within the "heavy SR" vesicles have a characteristic fiberlike appearance (Fig. 9*e*) with glutaraldehyde, with or without tannic acid. The terminal cisternae of the SR have the same fiberlike appearance *in situ* (Fig. 9*f*). That is to say, tannic acid only enhances the contrast but the appearance is otherwise similar (compare Fig. 9*e* and *f*).

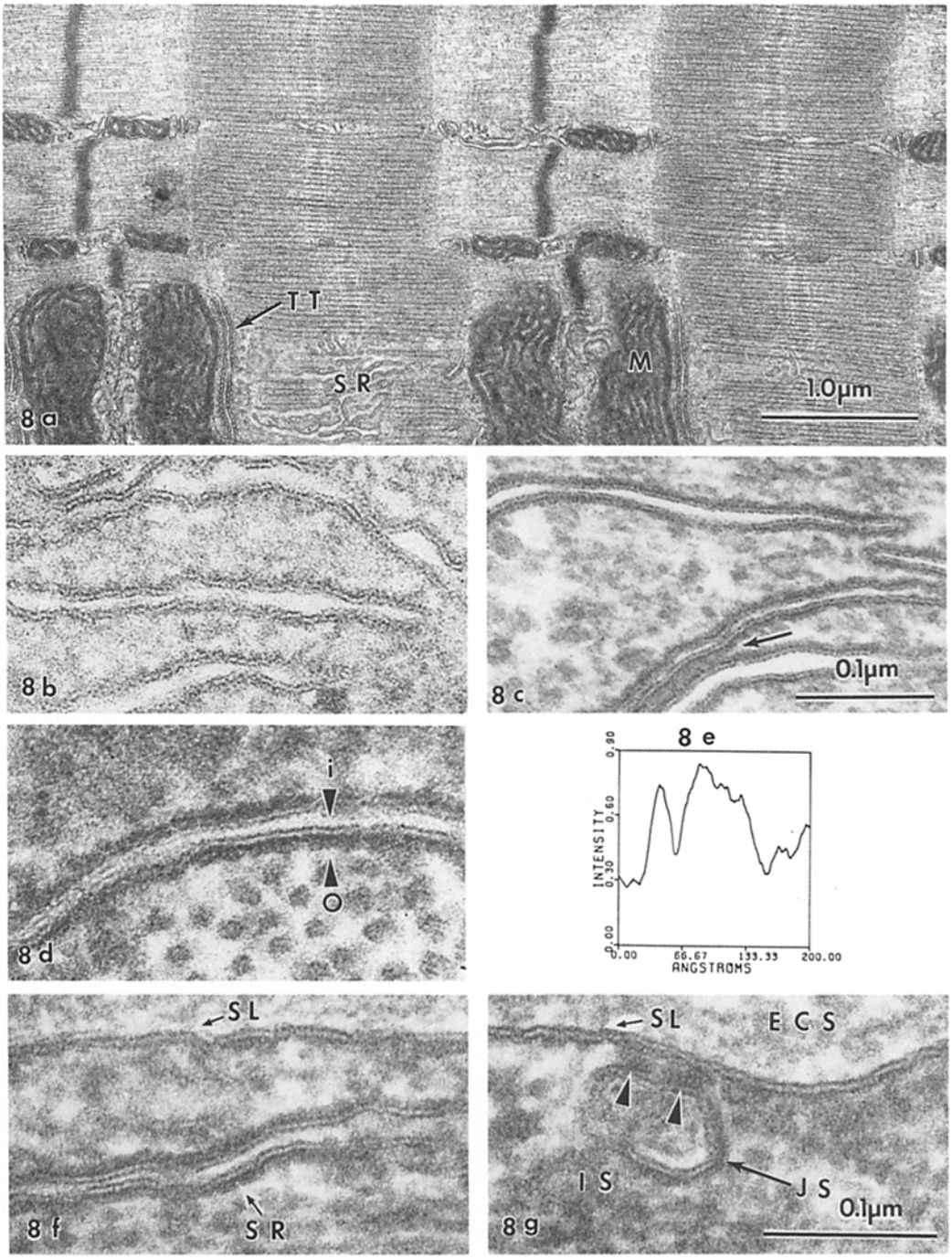

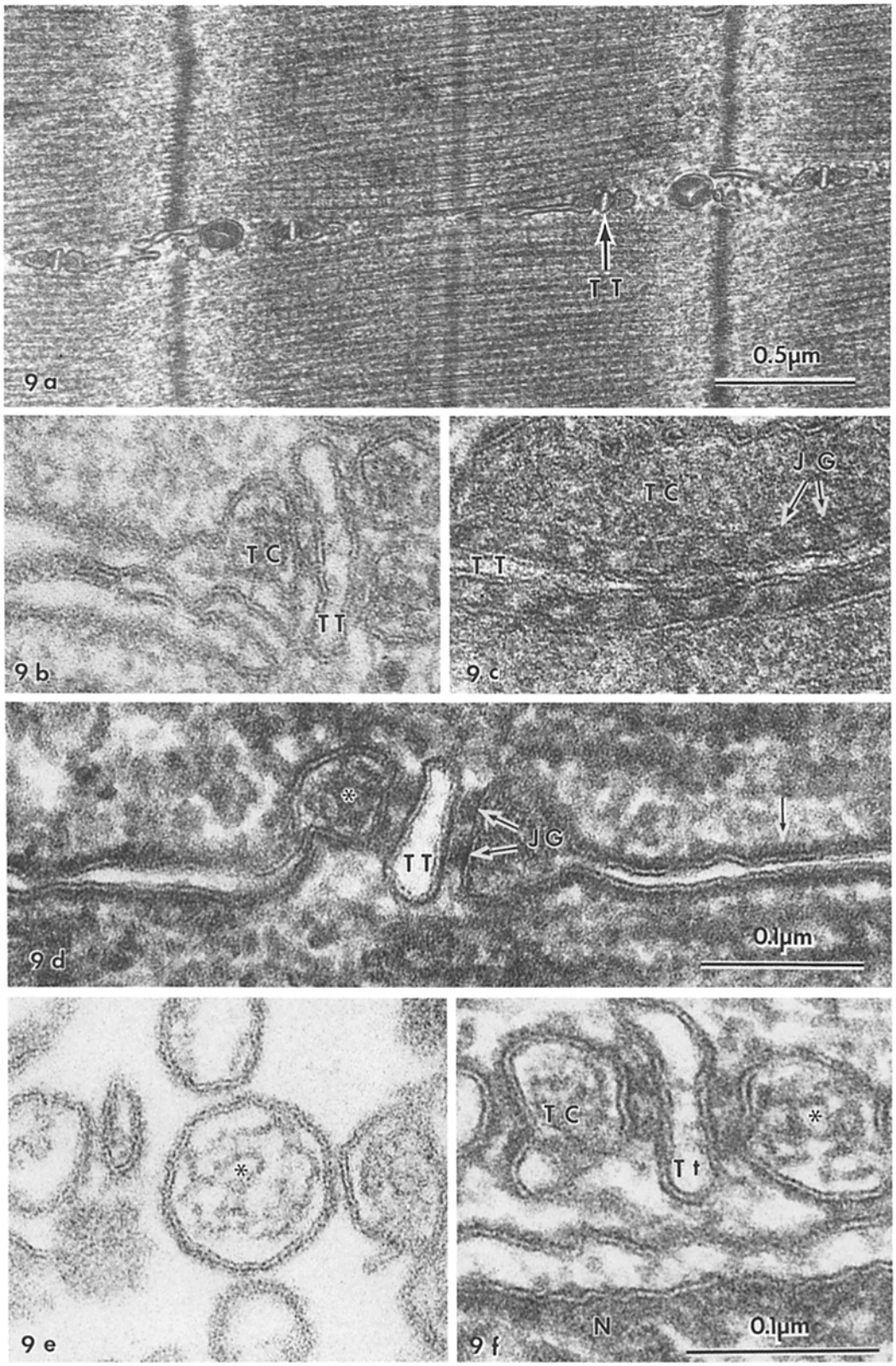
T T
0.5μm
9 a
T C
T T
9 b
T C
J G
T T
9 c
*
T T
J G
0.1μm
9 d
*
9 e
T C
T t
*
N
0.1μm
9 f

DISCUSSION

Tannic acid has been used to obtain enhanced contrast of isolated SR vesicles and muscle tissue in thin sections. The asymmetry of the sarcoplasmic membrane can now be impressively visualized both in isolated SR membrane vesicles and in muscle tissue sections. The enhanced contrast also allows better visualization of the SR-T-tubule junction (triad structure) including the dense material within the terminal cisternae as well as the junction granules, described by Franzini-Armstrong (8, 9).

Tannic acid has been applied to many different tissues to highlight and contrast a variety of structures such as microtubules, membranes, and membrane junctions (1, 2, 4, 10, 19, 30, 32, 36, 43). The mode of action of tannic acid has recently been studied (31, 42). Tannic acid consists mainly of low molecular weight esters of hexagalloylglucose which seems to penetrate readily when used together with glutaraldehyde or osmium tetroxide as fixative. The tannic acid seems to serve as a mordant between osmium-treated structures and lead, as well as to stabilize some tissue components against extraction resulting from dehydration and subsequent processing (41).

SR is a highly specialized membrane. Three proteins truly predominate in the highly purified sarcoplasmic reticulum preparation (25), of which the Ca^{++} pump protein, 119,000 daltons (35), accounts for ~70–75% of the protein (25). Isopycnic centrifugation allows further subfractionation yielding a continuum in which "light" and "heavy" SR are at the low and high density extremes of the gradient. Heavy SR is highly enriched with regard to the Ca^{++}-binding protein which, in large part, accounts for the dense material within its compartment (29). The SR is predominantly membrane, consisting mainly of Ca^{++} pump protein (~90% of the protein of the membrane). We have previously suggested that the heavy and light SR fractions are derived from the terminal and lateral cisternae, respectively, based on whether they contain electron-opaque contents (29). The present study further reinforces this suggestion whereby the dense contents of heavy SR and the terminal cisternae can be visualized with even greater contrast (compare Figs. 9*b* and *d*; *e* and *f*). More recently, the triad structure has been isolated and further subfractionated into heavy SR vesicles and T-tubules. The heavy SR vesicles, derived from the triads, have been found to be enriched in Ca^{++}-binding protein (20). We now find that the electron-opaque material both in the heavy SR and in the terminal cisternae of the triad, *in situ*, has similar fiberlike characteristics, further reinforcing the concept that heavy SR derive from the terminal cisternae (Fig. 9*e* and *f*).

The asymmetric structure of the SR membrane has previously been suggested by the visualization of 40-Å particles on the outer surface of the membrane, observed by negative staining (12, 13, 39). In the present study, we find, by negative staining, particles on both inner and outer surfaces of reconstituted SR (Fig. 3*c* and *e*), thereby further substantiating membrane asymmetry in the normal SR. Asymmetry is further suggested from freeze-fracture studies whereby most of the particles at the hydrophobic center appear in the concave (outer) fracture face (3, 33). The particles are distributed on both inner and outer fracture faces in reconstituted membranes (Fig. 7*b*).

The asymmetry of the SR membrane can now

FIGURE 9 Rabbit skeletal muscle in thin section with emphasis on the triad region. (*a*) Longitudinal section of rabbit skeletal muscle fixed with glutaraldehyde-OsO_4-tannic acid (× 60,000). The morphology of this tannic acid section is well preserved, and the enhanced contrast indicates that the tannic acid has penetrated well into the tissue. (*b, d,* and *f*) Cross-section of the triad region. (*c*) Longitudinal section of the triad. (*e*) Purified fraction of SR vesicles. Fig. 9*b* and *e* show muscle fixed with glutaraldehyde-OsO_4. Fig. 9*c, d,* and *f* show muscle fixed with glutaraldehyde-OsO_4-tannic acid. The magnification of Fig. 9*b, c,* and *d* is 250,000, and of Fig. 9*e* and *f* is 300,000. Tannic acid enhances contrast so that the asymmetry of the SR membrane is readily visualized (compare Fig. 9*b* and *d*). Transverse tubules (*TT*) can be visualized between terminal cisternae (*TC*) of the sarcoplasmic reticulum, the gaps being bridged by junction granules (*JG*). Note dense contents within the terminal cisternae but not in the transverse tubules or lateral cisternae. Tannic acid enhances the contrast of the junction granules (see *JG* arrows) and reveals the asymmetry of the SR membrane (compare Fig. 9*d* and *b*). Fibrous (~40 Å diameter) contents can be visualized in some isolated SR vesicles (Fig. 9*e*). The terminal cisternae (Fig. 9*f*) contain characteristic electron-opaque fibers similar to that visualized in "heavy" SR vesicles (Fig. 9*e*). The asterisks denote the fiberlike material within the terminal cisternae (*d*, *e*, and *f*).

be readily visualized in thin sections with the use of tannic acid; the outer broad band of the trilaminar membrane is 70 Å compared with the inner band which is 20 Å. We believe that the asymmetric appearance of the SR membrane is a true reflection of the membrane structure and does not result from the lack of penetration of the tannic acid, for the following reasons: (*a*) tryptic digestion of the membrane surface protein decreases the width of the outer broad band of the SR membrane (Fig. 2); (*b*) within the same section, the SR membrane appears highly asymmetric whereas the sarcolemma has a more symmetric appearance (Figs. 8*f* and *g*); (*c*) the asymmetry can be visualized in vesicles made leaky by an EDTA treatment (Fig. 5); (*d*) reconstituted SR membranes have a symmetric appearance containing both broad outer and inner bands (Figs. 6*c* and *e*); (*e*) membrane asymmetry can be visualized with glutaraldehyde, in the absence of tannic acid (Fig. 1*b*), albeit with poor contrast and irregular appearance. In spots, the outer band approaches 70 Å in width. This poorly visualized patching can now be interpreted in terms of membrane asymmetry as a matter of hindsight. Tannic acid enhances the contrast in the isolated SR and makes possible the visualization of membrane asymmetry in thin sections of muscle tissue. This is the first time that such asymmetry of SR could be observed in a muscle tissue section. In both isolated vesicles and SR, *in situ*, the orientation of the membrane is the same, i.e., the broad band is on the outside and anisotropic pumping of Ca^{++} is to the inside of the compartment.

A comparison of negative staining and thin section electron microscopy using tannic acid on normal and reconstituted SR is shown diagrammatically in Fig. 10. Normal SR is a highly asymmetric membrane that is visualized with either method of sample preparation, whereas the reconstituted membrane is symmetric containing broad inner and outer bands, ~70 Å wide. Negative staining shows distinct 40-Å round particles connected to the membrane by a narrow stalk ~10 Å long. Tannic acid does not reveal such molecular detail but rather an intense broad band of 70 Å, of which ~20 Å is referable to phospholipid; ~50 Å of this width must then be referable to protein extending from the bilayer of the membrane. Hence both methods reflect comparable asymmetry referable to the protein (compare Figs. 1, 3 and 6). When the width of the membrane is being measured by negative staining, care must be exercised to measure the limiting width. We interpret the broader width to result from incomplete flattening of the membrane on drying and/or due to lack of penetration of the stain. When such care is taken, the width of the SR membrane as viewed by negative staining is generally slightly narrower or, in the limit, equal to that viewed in thin-section electron microscopy using tannic acid.

The asymmetry of the SR is clearly referable to the shape and orientation of the Ca^{++} pump protein (cf. Figs. 10 and 11). The Ca^{++} pump protein, the major component of the SR mem-

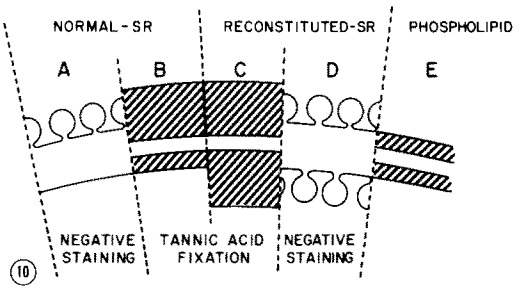

FIGURE 10 Diagrammatic representation of normal and reconstituted SR membranes as visualized by negative staining and in thin section electron microscopy using tannic acid. The 40-Å particles observed with negative staining (*A* and *D*) and the broadened outer band in thin section using tannic acid extend ~50 Å from the surface (*B* and *C*), compared with phospholipid (*E*). The membrane is asymmetric in normal SR (*A* and *B*) and symmetric in reconstituted membranes (*C* and *D*).

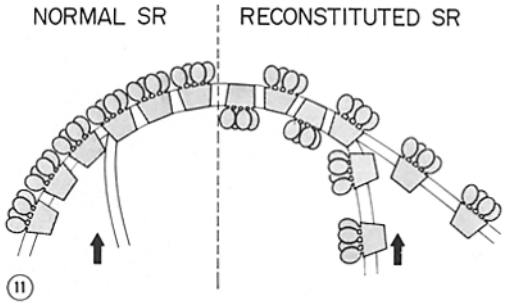

FIGURE 11 Diagrammatic representation of normal and reconstituted SR on the molecular level and the effect of freeze-fracture process on these membranes. The pumping unit is depicted as a tetramer consisting of four Ca^{++} pump protein molecules (see text). According to this representation, the Ca^{++} pump is unidirectionally aligned (head groups extend from outer surface) in normal SR and facing both directions in reconstituted vesicles. The ratio of surface particles visualized by negative staining to intramembrane particles observed by freeze-fracture would be four to one.

brane, has the key requisites to be the Ca^{++}-pumping machinery: it (*a*) contains two specific Ca^{++}-binding sites and one ATP-binding site (26); (*b*) contains Ca^{++}-stimulated ATPase activity which undergoes a two-step reaction, formation of a phosphoenzyme intermediate and its breakdown (16, 23); (*c*) can be incorporated into membranes which are then capable of energized pumping of Ca^{++} (27, 28, 34).

The Ca^{++} and ATP react on the outer surface of the SR membrane, and it is therefore reasonable to expect that the specific Ca^{++}- and ATP-binding sites be localized on the outer surface of the membrane. It was surprising therefore that, at 120 h of trypsin digestion of SR vesicles, the surface particles observed by negative staining were no longer visible, yet the ATPase activity had doubled. In this regard, two points are relevant: (*a*) the Ca^{++}-stimulated ATPase activity is latent and is not a reliable measure of the amount of Ca^{++} pump protein (M. Pilarska and S. Fleischer. Unpublished studies. See also references 13, 28, and 39); (*b*) smaller fragments of the Ca^{++} pump protein retain ATPase activity and may remain on the surface of the membrane after the 40-Å surface particles are no longer visible (13, 39).

The number of surface particles observed by negative staining is several fold greater than the number of intramembrane particles observed by freeze-fracture electron microscopy (13, 14, 18, 22). A diagrammatic representation of the orientation of the Ca^{++} pump in normal and reconstituted SR membranes is shown in Fig. 11. Each Ca^{++} pump protein molecule is visualized to consist of three portions, i.e. a head piece (~40 Å), a narrow neck (~10 Å), and a tail region (~60 Å) accounting for a total width of the membrane of ~110 Å. The pumping unit is depicted as a tetramer consisting of four Ca^{++} pump molecules associated at the tail region to form a single base piece, while the four head pieces extend from the outer surface of the membrane. The base piece is visualized as an intramembrane particle by freeze-fracture electron microscopy, whereas the head pieces extend from the membrane surface as observed by negative staining electron microscopy. The base piece may form a channel through which the Ca^{++} is translocated whereas the Ca^{++}- and ATP-binding sites may be at the head or neck regions. In reconstituted membranes, the pumps are randomly aligned with the polar head groups extending from both inner and outer surfaces. Nonetheless, reconstituted SR is capable of unidirectional pumping of Ca^{++} because asymmetry is imposed by addition of the substrates, Ca^{++} and ATP, to the medium. Only those pump molecules whose head portions extend from the outer surface of the membrane into the medium would react with substrate to pump Ca^{++} anisotropically into the lumen of the vesicle.

We are grateful to Dr. Charles Auer for obtaining the densitometry tracings and to Mrs. Christine Dettbarn for capable technical assistance.

These studies were supported in part by grants from the National Institutes of Health (AM 14632) and the Muscular Dystrophy Associations of America, Inc.

Received for publication 20 March 1978, and in revised form 24 July 1978.

REFERENCES

1. Burton, P. R., R. E. Hinkley, and G. B. Pierson. 1975. Tannic acid-stained mictotubules with 12, 13, 15 protofilaments. *J. Cell Biol.* **65**:227–233.
2. Bonilla, E. 1977. Staining of transverse tubular system of skeletal muscle by tannic acid-glutaraldehyde fixation. *J. Ultrastruct. Res.* **58**:162–165.
3. Deamer, D. W., and R. J. Baskin. 1969. Ultrastructure of sarcoplasmic reticulum preparations. *J. Cell Biol.* **42**:296–307.
4. Deurs, B. V. 1975. The use of a tannic acid-glutaraldehyde fixative to visualize gap and tight junctions. *J. Ultrastruct. Res.* **50**:185–192.
5. Duggan, P. F., and A. Martonosi. 1970. Sarcoplasmic reticulum: IX. The permeability of sarcoplasmic reticulum membranes. *J. Gen. Physiol.* **56**:147–167.
6. Fiske, C. H., and Y. Subbarow. 1925. Colorometric determination of phosphorus. *J. Biol. Chem.* **66**:375–400.
7. Fleischer, S., B. Fleischer, and W. Stoeckenius. 1967. Fine structure of lipid-depleted mitochondria. *J. Cell Biol.* **32**:193–208.
8. Franzini-Armstrong, C. 1970. Studies of the triad. I. Structure of the junction in frog twitch fibers. *J. Cell Biol.* **47**:488–499.
9. Franzini-Armstrong, C. 1975. Membrane particles and transmission at the triad. *Fed. Proc.* **34**:1382–1389.
10. Futaesaku, Y., V. Mizuhira, and H. Nakamura. 1972. A new fixation method using tannic acid for electron microscopy and some observations of biological specimens. *Proc. Int. Congr. Histochem. Cytochem.* **4**:155–156.
11. Ikemoto, N., G. M. Bhatnagar, B. Nagy, and J. Gergely. 1972. Interaction of divalent cations with the 55,000-dalton protein component of the sarcoplasmic reticulum. Studies of fluorescence and circular dichroism. *J. Biol. Chem.* **247**:7835–7837.
12. Ikemoto, N., F. A. Sreter, and A. Nakamura. 1968. Tryptic digestion and localization of calcium uptake and ATPase activity in fragments of sarcoplasmic reticulum. *J. Ultrastruct. Res.* **23**:216–222.
13. Inesi, G., and D. Scales. 1974. Tryptic cleavage of sarcoplasmic reticulum protein. *Biochemistry.* **13**:3298.
14. Inesi, G., and D. Scales. 1976. Assembly of ATPase protein in sarcoplasmic reticulum membranes. *Biophys. J.* **16**:735–751.
15. Kalina, M., and D. C. Pease. 1977. The probably role of phosphatidylcholines in the tannic acid enhancement of cytomembrane electron contrast. *J. Cell Biol.* **74**:742–746.
16. Kamazawa, T., S. Yamada, T. Yamamoto, and Y. Tonomura. 1971. Reaction mechanism of the Ca^{2+}-dependent ATPase of sarcoplasmic reticulum from skeletal muscle. V. Vectorial requirements for calcium and magnesium ions of three partial reactions of ATPase: formation and decomposition of a phosphorylated intermediate and ATP-formation from ADP and the intermediate. *J. Biochem. (Tokyo).* **70**:95–123.
17. Laemmli, U. K. 1970. Cleavage of structural proteins during assembly of the head of bacteriophage T4. *Nature (Lond.).* **227**:680–685.
18. Jilka, R. L., A. N. Martonosi, and T. W. Tillock. 1975. Effect of purified [Mg^{2+} + Ca^{+2}]-activated ATPase of sarcoplasmic reticulum upon the passive permeability and ultrastructure of phospholipid vesicles. *J. Biol. Chem.* **250**:7511–7524.

19. LAFOUNTAIN, J. R., JR., C. R. ZOBEL, H. R. THOMAS, and C. GALBREATH. 1977. Fixation and staining of F-actin and microfilaments using tannic acid. *J. Ultrastruct. Res.* **58:**78–86.
20. LAU, Y. H., A. H. CASWELL, and J.-P. BRUNSCHWIG. 1977. Isolation of transverse tubules by fractionation of triad junctions of skeletal muscle. *J. Biol. Chem.* **252:**5565–5574.
21. LOWRY, O. H., N. J. ROSEBROUGH, A. L. FARR, and R. J. RANDALL. 1951. Protein measurement with the Folin phenol reagent. *J. Biol. Chem.* **193:**265–275.
22. MALAN, N. T., R. SABBADINI, D. SCALES, and G. INESI. 1975. Functional and structural roles of sarcoplasmic reticulum functional components. *FEBS (Fed. Eur. Biochem. Soc.) Letters.* **60:**122–125.
23. MAKINOSE, M. 1973. Possible functional state of the enzyme of the sarcoplasmic calcium pump. *FEBS (Fed. Eur. Biochem. Soc.) Letters.* **37:**140–143.
24. MEISSNER, G., and S. FLEISCHER. 1971. Characterization of sarcoplasmic reticulum from skeletal muscle. *Biochim. Biophys. Acta.* **241:**356–378.
25. MEISSNER, G., G. E. CONNER, and S. FLEISCHER. 1973. Isolation of sarcoplasmic reticulum by zonal centrifugation and purification of Ca^{++} pump and Ca^{++} binding protein. *Biochim. Biophys. Acta.* **298:**246–269.
26. MEISSNER, G. 1973. ATP and Ca^{++} binding by the Ca^{++} pump protein of sarcoplasmic reticulum. *Biochim. Biophys. Acta.* **298:**906–926.
27. MEISSNER, G., and S. FLEISCHER. 1973. Ca^{2+} uptake in reconstituted sarcoplasmic reticulum vesicles. *Biochem. Biophys. Res. Commun.* **52:**913–919.
28. MEISSNER, G., and S. FLEISCHER. 1974. Dissociation and reconstitution of functional sarcoplasmic reticulum vesicles. *J. Biol. Chem.* **249:**302–309.
29. MEISSNER, G. 1975. Isolation and characterization of two types of sarcoplasmic reticulum vesicles. *Biochim. Biophys. Acta.* **389:**51–68.
30. MIZUHIRA, V., and Y. FUTAESAKU. 1971. On the new approach of tannic acid and digitonin to the biological fixatives. *Proc. Electron Microsc. Soc. Am.* **29:**494.
31. MIZUHIRA, V., and Y. FUTAESAKU. 1972. New fixation for biological membranes using tannic acids. *Akta Histochem. Cytochem.* **5:**233–234.
32. MOLLENHAUER, H. H., D. J. MORRE, and B. S. HASS. 1977. Plasma membrane transformations in spermatogenesis revealed by aldehyde fixatives containing tannic acid. *J. Ultrastruct. Res.* **61:**166–171.
33. PACKER, L., C. W. MEHARD, G. MEISSNER, W. L. ZAHLER, and S. FLEISCHER. 1974. The structural role of lipids in mitochondrial and sarcoplasmic reticulum membranes. Freeze-fracture electron microscopy studies. *Biochim. Biophys. Acta.* **363:**159–181.
34. RACKER, E. 1972. Reconstitution of a calcium pump with phospholipids and purified Ca^{++}-adenosine triphosphatase from sarcoplasmic reticulum. *J. Biol. Chem.* **247:**8198–8200.
35. RIZZOLO, L. J., M. LEMAIRE, J. A. REYNOLDS, and C. TANFORD. 1976. Molecular weights and hydrophobicity of the polypeptide chain of sarcoplasmic reticulum calcium (II) adenosine triphosphatase and its primary tryptic fragments. *Biochemistry.* **15:**3433–3437.
36. ROSEWALD, R., and M. J. KARNOVSKY. 1974. Porous substructure of the glomerular slit diaphragm in the rat and mouse. *J. Cell Biol.* **60:**423–433.
37. SAITO, A., C. T. WANG, and S. FLEISCHER. 1977. Ultrastructure of normal and reconstituted sarcoplasmic reticulum membranes viewed in thin section using tannic acid fixation. *J. Cell Biol.* **75:**220*a*. (Abstr.)
38. SATO, T. 1968. A modified method for lead staining of thin sections. *J. Electron Microsc.* **17:**158–159.
39. STEWART, P. S., and D. H. MACLENNAN. 1974. Surface particles of sarcoplasmic reticulum membranes. Structural features of the adenosine triphosphatase. *J. Biol. Chem.* **249:**985–993.
40. STEWART, P. S., D. H. MACLENNAN, and A. E. SHAMOO. 1976. Isolation and characterization of tryptic fragments of the adenosine triphosphate of sarcoplasmic reticulum. *J. Biol. Chem.* **251:**712–719.
41. SIMIONESCU, N., and M. SIMIONESCU. 1976. Galloylglucoses of low molecular weight as mordant in electron microscopy. *J. Cell Biol.* **70:**608–621.
42. SIMIONESCU, M., N. SIMIONESCU, and G. E. PALADE. 1975. Segmental differentiations of cell junctions in the vascular endothelium. *J. Cell Biol.* **67:**863–885.
43. TILNEY, L. G., J. BRYAN, and D. J. BUSH. 1973. Microtubules: evidence for 13 protofilaments. *J. Cell Biol.* **59:**267.
44. YU, B. P., E. J. MASORO, and T. F. MORLEY. 1976. Analysis of the arrangement of protein components in the sarcoplasmic reticulum of rat skeletal muscle. *J. Biol. Chem.* **251:**2037–2043.